



UvA-DARE (Digital Academic Repository)

Cobalt-Catalyzed Hydrogenations via Olefin Cobaltate and Hydride Intermediates

Sandl, S.; Maier, T.M.; van Leest, N.P.; Kröncke, S.; Chakraborty, U.; Demeshko, S.; Koszinowski, K.; de Bruin, B.; Meyer, F.; Bodensteiner, M.; Herrmann, C.; Wolf, R.; Jacobi von Wangelin, A.

DOI

[10.1021/acscatal.9b01584](https://doi.org/10.1021/acscatal.9b01584)

Publication date

2019

Document Version

Final published version

Published in

ACS Catalysis

License

Article 25fa Dutch Copyright Act

[Link to publication](#)

Citation for published version (APA):

Sandl, S., Maier, T. M., van Leest, N. P., Kröncke, S., Chakraborty, U., Demeshko, S., Koszinowski, K., de Bruin, B., Meyer, F., Bodensteiner, M., Herrmann, C., Wolf, R., & Jacobi von Wangelin, A. (2019). Cobalt-Catalyzed Hydrogenations via Olefin Cobaltate and Hydride Intermediates. *ACS Catalysis*, 9(8), 7596-7606. <https://doi.org/10.1021/acscatal.9b01584>

General rights

It is not permitted to download or to forward/distribute the text or part of it without the consent of the author(s) and/or copyright holder(s), other than for strictly personal, individual use, unless the work is under an open content license (like Creative Commons).

Disclaimer/Complaints regulations

If you believe that digital publication of certain material infringes any of your rights or (privacy) interests, please let the Library know, stating your reasons. In case of a legitimate complaint, the Library will make the material inaccessible and/or remove it from the website. Please Ask the Library: <https://uba.uva.nl/en/contact>, or a letter to: Library of the University of Amsterdam, Secretariat, Singel 425, 1012 WP Amsterdam, The Netherlands. You will be contacted as soon as possible.

UvA-DARE is a service provided by the library of the University of Amsterdam (<https://dare.uva.nl>)

Cobalt-Catalyzed Hydrogenations via Olefin Cobaltate and Hydride Intermediates

Sebastian Sandl,[†] Thomas M. Maier,[‡] Nicolaas P. van Leest,[§] Susanne Kröncke,[†] Uttam Chakraborty,[†] Serhiy Demeshko,^{||} Konrad Koszinowski,[⊥] Bas de Bruin,[§] Franc Meyer,^{||} Michael Bodensteiner,[‡] Carmen Herrmann,[†] Robert Wolf,^{*,‡,||} and Axel Jacobi von Wangelin^{*,†,||}

[†]Department of Chemistry, University of Hamburg, Martin Luther King Pl 6, 20146 Hamburg, Germany

[‡]Institute of Inorganic Chemistry, University of Regensburg, 93040 Regensburg, Germany

[§]van't Hoff Institute for Molecular Sciences, University of Amsterdam, Science Park 904, 1098 XH Amsterdam, The Netherlands

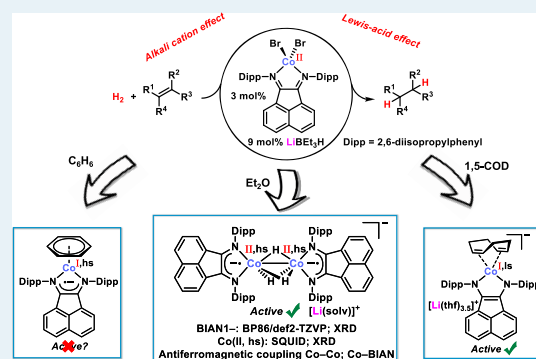
^{||}Institute of Inorganic Chemistry, Universität Göttingen, Tammannstrasse 4, 37077 Göttingen, Germany

[⊥]Institute of Organic and Biomolecular Chemistry, Universität Göttingen, Tammannstrasse 2, 37077 Göttingen, Germany

Supporting Information

ABSTRACT: Redox noninnocent ligands are a promising tool to moderate electron transfer processes within base-metal catalysts. This report introduces bis(imino)acenaphthene (BIAN) cobaltate complexes as hydrogenation catalysts. Sterically hindered trisubstituted alkenes, imines, and quinolines underwent clean hydrogenation under mild conditions (2–10 bar, 20–80 °C) by use of the stable catalyst precursor [(DⁱPPBIAN)CoBr₂] and the cocatalyst LiEt₃BH. Mechanistic studies support a homogeneous catalysis pathway involving alkene and hydrido cobaltates as active catalyst species. Furthermore, considerable reaction acceleration by alkali cations and Lewis acids was observed. The dinuclear hydridocobaltate anion with bridging hydride ligands was isolated and fully characterized.

KEYWORDS: hydrogenation, cobalt, hydrides, metalloradicals, reaction mechanism, redox-active ligands



INTRODUCTION

Metal-catalyzed hydrogenations of alkenes constitute one of the key chemical transformations with numerous applications to lab-scale syntheses and industrial manufacturing.¹ The elucidations of the underlying catalytic mechanisms by Eisenberg, Halpern, Tolman, and others were major scientific milestones towards the understanding of catalytic elemental steps and the rational design of more active and selective catalysts.^{1,2} Very recently, the dominance of hydrogenation catalysts based on the noble metals Rh, Ru, Ir, Pd, and Pt has been challenged by the development of highly active 3d transition metals.³ While the use of more abundant, cheaper, and often less toxic base metals constitutes an important contribution to a more sustainable chemistry, their distinct reactivity and selectivity was often plagued by undesirable destructive side reactions.⁴ Recently, elaborate ligand design enabled the development of highly active cobalt catalysts by the groups of Beller, Budzelaar, Chirik, Hanson, Elsevier, de Bruin, and others (Figure 1).^{5–8} In the most recent literature, the implementation of pincer ligands (e.g., NNN; PNP; CNC) proved pivotal to the control of high activity and selectivity.⁹ Following our previous work on metalates with redox noninnocent arene ligands,^{10,11} we believed that an efficient 3d metal catalyst for hydrogenation reactions would fulfill the

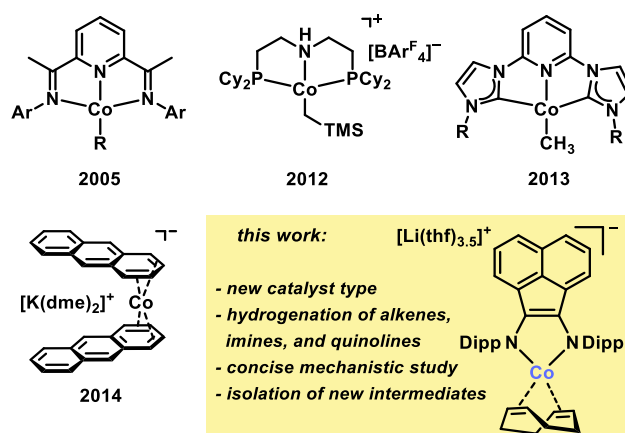


Figure 1. Homogeneous cobalt catalysts for hydrogenations^{8a–c,10} (Dipp = 2,6-diisopropylphenyl).

following criteria: (i) facilitation of redox steps at the metal by a redox-active ligand; (ii) modular ligand design that allows for

Received: April 24, 2019

Revised: July 2, 2019

Published: July 10, 2019

convenient synthesis and easy catalyst tuning; (iii) stabilization of reduced forms of the catalyst by the ligand, and (iv) broad scope of hydrogenations of unsaturated C=C and C=X bonds.

Imine-based ligand architectures constitute a privileged class of ligands as evidenced by the numerous applications to catalytic reactions.⁷ Simple α -diimine catalysts were first introduced by *tom Dieck* and co-workers in 1977.¹² Pincer-type motifs such as pyridinediimines¹³ (PDI) have recently received great attention. Bis(imino)acenaphthenes^{14,15} (BIANs) are another class of ligands that fulfill the aforementioned criteria: BIANs can be rapidly assembled from commercial precursors on multigram scales and are highly redox-active as they can harbor up to four electrons.^{14b} There are eight reports of BIAN cobalt complexes with five applications to catalysis.¹⁶ On this basis, we investigated combinations of BIAN ligands and cobalt salts toward their ability to form active hydrogenation catalysts. Documented herein are the benefits of using this simple catalytic system that presents tangible advances over the current state-of-the-art that could not have been predicted: Clean hydrogenations of challenging alkenes (e.g., tetra-substituted), imines, and heteroarenes proceed under mild conditions. Mechanistic insight was gained from the isolation of structurally novel olefin and hydride complexes as potential catalyst intermediates that are distinct from those of the traditional noble metal catalysts (Figure 1, bottom).

RESULTS AND DISCUSSION

Optimization and Alkene Hydrogenation. Initially, we probed the ability of $(\text{D}^{\text{ipp}}\text{BIAN})\text{Co}^{\text{II}}\text{Br}_2$ to act as a precatalyst for the hydrogenation of the model substrate triphenylethylene under very mild conditions (Dipp = 2,6-diiso-propylphenyl). High conversion was observed with lithium superhydride (LiEt_3BH) as a cocatalyst at 2 bar H_2 and room temperature with only 3 mol % $(\text{D}^{\text{ipp}}\text{BIAN})\text{CoBr}_2$ (Table 1, procedure A). The presence of olefins during the reduction proved beneficial for the high catalyst activity, possibly due to transient olefin coordination and stabilization of the low-valent catalyst.^{6d,17,18} The significantly lower activity of NaEt_3BH suggests a considerable alkali-cation effect (entry 5; Supporting Information (SI)).¹⁹ Mono-, di-, and trisubstituted alkenes were cleanly hydrogenated under 2–10 bar H_2 pressure at room temperature (Scheme 1).²⁰ The high efficacy of the developed protocol was demonstrated in the hydrogenation of challenging tri- and tetra-substituted alkenes such as myrcene, α -pinene, and α,β,β -trimethylstyrene under mild conditions (Scheme 2). Under standard conditions, the hydrogenation of α -methylstyrene exhibited a turnover frequency (TOF) of 780 h^{-1} (Supporting Information). To the best of our knowledge, this protocol involves one of the most active homogeneous Co catalysts for alkene hydrogenations.⁸ Reduction-sensitive functional groups in the alkenes required a different protocol involving addition of the hydride cocatalyst prior to the alkene (protocol B, see Table 1, entry 2, and Scheme 2, right). This alternative protocol B was tolerant to chloride, bromide, ether, and ester functions. In the absence of H_2 , 1-octene rapidly isomerized to a mixture of octene regioisomers and stereoisomers. With phenyl-acetylene, slow cyclotrimerization to triphenylbenzene was observed in low yield (see the Supporting Information).²¹

Methodology Extension: Hydrogenation of Imines. The homogeneous Co-catalyzed hydrogenation of imines^{8b,10}

Table 1. Selected Optimization Experiments^b

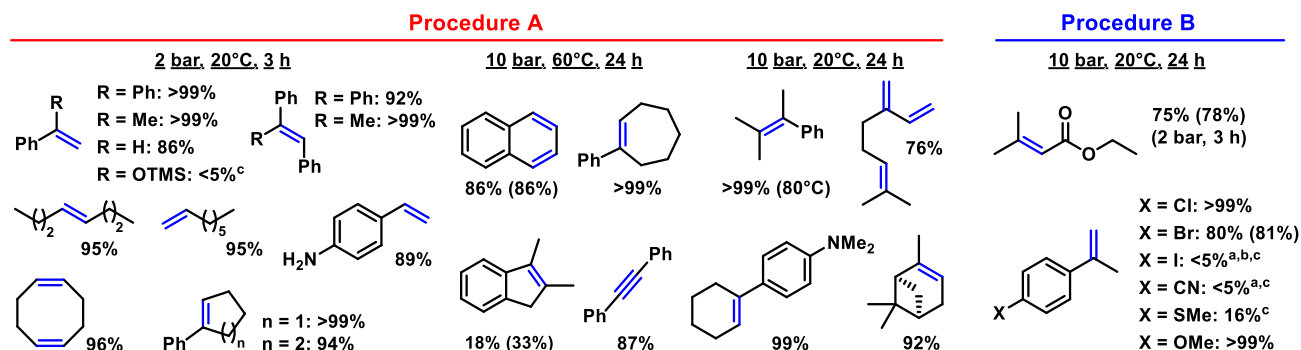
Entry	Deviation from standard conditions	Yield (%) ^a
1	A: reduction in presence of the substrate	92 (93)
2	B: substrate addition after reductant	41 (50)
3	A: 6 mol% LiEt_3BH	75 (75)
4	A: 6 mol% NaEt_3BH	23 (33)
5	A: 9 mol% NaEt_3BH	64 (65)
6	A: 9 mol% HBpin + 9 mol% KO^tBu	1 (12)
7	A: $(\text{D}^{\text{ipp}}\text{BIAN})\text{CoCl}_2$	72 (72)
8	A: CoCl_2 + 2 $\text{D}^{\text{ipp}}\text{BIAN}$	25 (35)
9	A: w/o reductant	<1 (9)

^aYields determined by quantitative GC-FID vs internal *n*-pentadecane; conversions in parentheses. ^bConditions: 0.2 mmol alkene (1 M, THF), 9 mol % LiEt_3BH (1 M, THF), 3 mol % $(\text{D}^{\text{ipp}}\text{BIAN})\text{CoBr}_2$, 2 bar H_2 .

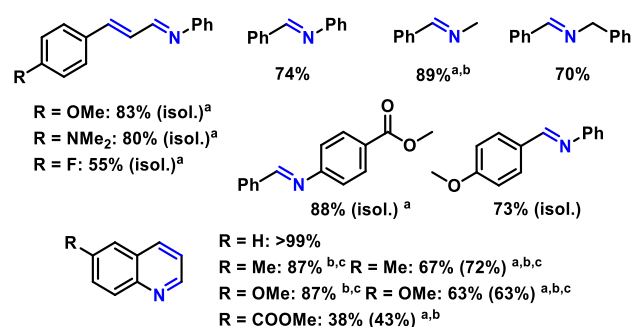
and quinolines^{8f,h} is still in its infancy, despite being an atom-economic route to bioactive amines.²² Very good conversions were observed with the same cobalt catalyst in hydrogenations of selected electron-deficient and electron-rich imines and quinolines (10 bar H_2 , 60 °C, Scheme 2). Ester functions were tolerated. Similarly mild conditions were recently reported with related homogeneous Co catalysts.^{8b,f,h,10}

Mechanism. The advent of 3d transition metal catalysts has gone hand in hand with the utilization of ligands that profoundly influence the electronic properties at the metal ions and enable redox reactivity patterns that are distinct from those of noble metals catalysts.⁹ The reaction mechanisms of catalytic alkene hydrogenations with second and third row transition metals (Rh, Ru, Ir, Pd, Pt) are very well understood. For the classical Rh-catalyzed hydrogenation, alkene and hydride complexes have been determined as key catalyst intermediates and the elemental reaction steps to involve two electron redox events at the metal.^{1,2,7,8} There is much less insight into the hydrogenation mechanisms of first row transition metals; the nature of the key catalyst intermediates are still largely unexplored. Chirik and co-workers reported on a bis(aryl-imidazol-2-ylidene)pyridine cobalt hydride complex and a radical pathway that operates in cobalt-catalyzed alkene hydrogenations.^{8c} In this work, we aimed at a concise mechanistic study of Co-BIAN catalysts in alkene hydrogenations that would address the following questions: Is the BIAN ligand redox-active under the reaction conditions?⁹ Are radical pathways operating?⁷ To what extent are heterogeneous catalyst species involved?²³ Do alkene and hydride intermediates play a similarly important role as with 4d and 5d metal catalysts?

We commenced our mechanistic studies with a set of key experiments that addressed the operation of radical mechanisms and the topicity of the active catalysts species. Initially,

Scheme 1. Substrate Scope of Cobalt-Catalyzed Hydrogenation of Alkenes^d

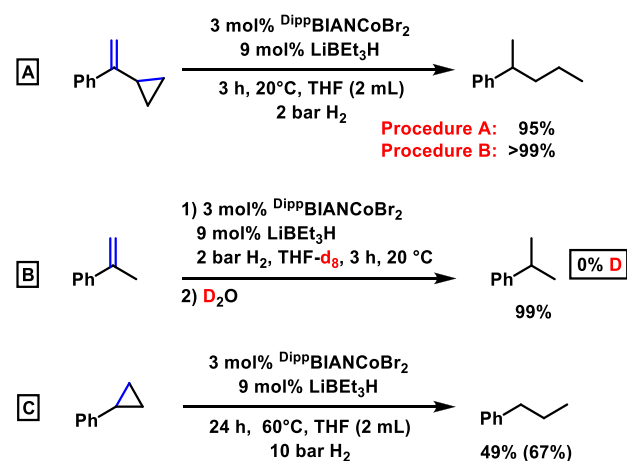
^aTraces of α -methylstyrene formed. ^bTraces of cumene formed. ^cConversion <20%. ^dBonds in blue indicate the site of complete π -bond hydrogenation. Standard conditions: 0.2 mmol alkene/alkyne (1 M, THF), 3 mol % (DⁱP^pBⁱAN)CoBr₂, 9 mol % LiEt₃BH (1 M, THF). Yields were determined by quantitative GC-FID vs *n*-pentadecane. Conversions are given in parentheses if <90%. Procedure A: catalyst reduction in the presence of substrate. Procedure B: catalyst reduction in the absence of substrate.

Scheme 2. Hydrogenation of Imines and Quinolines^d

^aProcedure B. ^b80 °C. ^cTraces of the 5,6,7,8-tetrahydroquinoline derivative. ^dBlue bonds indicate the sites of double bond hydrogenation. Conditions: procedure A, 0.2 mmol substrate (1 M, THF), 3 mol % (DⁱP^pBⁱAN)CoBr₂, 9 mol % LiEt₃BH (1 M, THF); 10 bar H₂, 60 °C, 24 h. GC-FID yields vs internal *n*-pentadecane; conversions in parentheses if <90%.

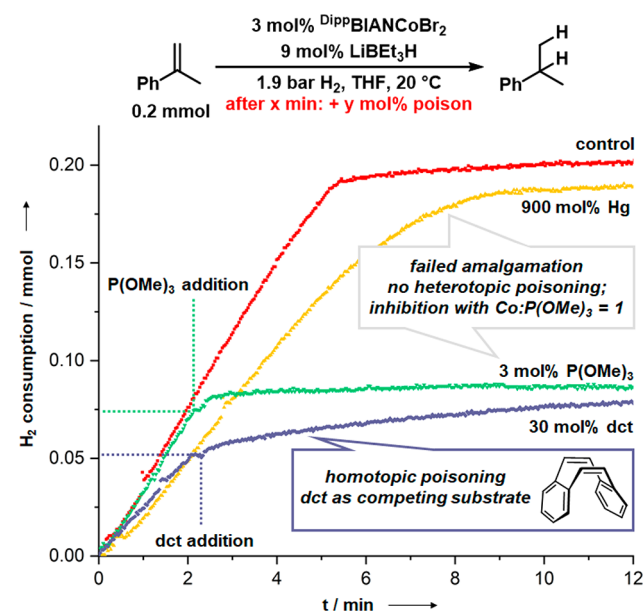
radical probes were evaluated. α -Cyclopropyl styrene underwent dual alkene hydrogenation and hydrogenative ring-opening to give 2-phenylpentane in excellent yields following protocol A or B, respectively (Scheme 3A). This might be indicative of a mechanism involving hydrogen atom transfer (HAT).²⁴ Furthermore, this is in full accord with our

Scheme 3. Key Mechanistic Experiments



observations that nonstyrenic olefins (i.e., alkenes without aryl substituents that could stabilize potential radical intermediates in benzyl positions) constitute more difficult substrates under the standard conditions. Hydrogen atom transfer from the solvent is rather unlikely as no deuterium incorporation could be determined from reactions in THF-*d*₈ (Scheme 3B). The high activity of the catalyst was further demonstrated by the hydrogenation of a C–C σ -bond in cyclopropylbenzene (Scheme 3C).

The clear distinction between homogeneous and heterogeneous catalyst species is intricate,²³ yet our observations are consistent with a homogeneous mechanism. Reaction progress analyses documented an immediate onset of catalytic activity and steady conversion, which indicates a zero order for the substrate in the rate law (Scheme 4, red curve). Thus, the rate-determining step presumably does not include olefin coordination. A plot of the initial rates versus catalyst

Scheme 4. Catalyst Poisoning Studies with P(OMe)₃, Hg, and dct^a

^aProcedure B. substrate conversion determined by gas-uptake and quantitative GC-FID vs *n*-pentadecane.

concentrations showed a first order rate in cobalt (SI). The absence of any sigmoidal curvature argues clearly against initial precatalyst nucleation and particle formation.⁶ However, an induction period might be not visible due to the experimental setup (procedure B, substrate conversion determined by gas-uptake; H₂ consumption was recorded after precatalyst formation and substrate addition; SI). Kinetic poisoning studies are a competent tool to ascertain the toxicity of the operating catalyst species.²³ The attempted amalgamation of the catalyst with 300 equiv. Hg had only a minimal effect on the reaction rate. Upon addition of subcatalytic amounts of trimethylphosphite (P(OMe)₃, 0.3 mol %), partial catalyst inhibition was recorded. Complete inhibition was achieved at a catalyst/poison ratio of 1:1 which is consistent with a homotopic catalyst (Scheme 4, green curve). The selective homotopic catalyst poison dibenzo[*a,e*]cyclooctatetraene²⁵ (dct, 10 equiv per Co) resulted in catalyst inhibition which was slightly diminished by the concomitant hydrogenation of dct as a competing substrate (Scheme 4, violet curve, 31% conversion of dct; SI). The lower efficacy of dct as poison is presumably a consequence of the lower stability of 3d olefin complexes vs their heavier congeners.¹⁸

Complexes and Catalyst Intermediates. Based on the initial mechanistic experiments, we postulate a homotopic mechanism by molecular cobalt catalysts. The distinct electronic properties of 3d transition metals vs their heavier congeners might also entail the participation of catalyst structures that are different from the Rh(I) catalysts of hydrogenation reactions. While the operation of alkene and hydride pathways has been intensively studied in rhodium-catalyzed hydrogenations, the knowledge of related catalyst intermediates with cobalt is still rather in its infancy. In an effort to identify potential catalyst species, we investigated reactions of (DⁱPPBIAN)CoBr₂ with 3 equiv LiEt₃BH in THF solution (Scheme 5). LIFDI-MS (liquid injection field desorption mass spectrometry) analyses of the crude catalyst mixture displayed the formation of the low-valent dimer [(DⁱPPBIAN)Co]₂ which is structurally related to a complex with two direct cobalt-arene bonding interactions prepared by Yang and co-workers using a different diimine.²⁶ We surmised that the low-valent monomeric unit (DⁱPPBIAN)Co might exhibit catalytic activity and thus employed several arenes/olefins as labile coordination placeholders during the reductive dehalogenation of (DⁱPPBIAN)CoBr₂. Reduction of (DⁱPPBIAN)CoBr₂ in THF with 3 equiv LiEt₃BH and excess amounts of 1,5-cyclooctadiene (cod) led to the formation of [Li(thf)₃]{(DⁱPPBIAN)Co(cod)} (1) which was isolated after recrystallization in 17% yield.^{27,16c} This complex is the corresponding Li salt to our previously described potassium cobaltate (2) and shows similar ¹H and ¹³C spectra.^{16c} Based on literature precedents, the oxidation level of BIAN in 1 can be assigned as 2- from the crystallographic bond distances (C–C: 1.389(4) Å; C–N: 1.383(3) Å; Figure 2).^{28,29} In comparison, (DⁱPPBIAN)CoBr₂ consists of a neutral BIAN (C–C: 1.513(7) and 1.521(6) Å; C–N: 1.277(7)–1.286(8) Å).^{16b,28,29}

The analogous reduction of (DⁱPPBIAN)CoBr₂ with 3 equiv LiEt₃BH in benzene furnished the neutral complex [(DⁱPPBIAN)Co(η⁶-C₆H₆)] (3) as dark red single crystals in 64% yield. (3 is also formed from the same reaction in a mixture of 1,5-cod and benzene).³⁰ Single crystal structure analysis suggests a radical anion state of the BIAN ligand (C–C 1.433(2) Å; C–N 1.3246(19) Å and 1.3224(19) Å, Figure

Scheme 5. Cobalt Complexes 1, 3, and 4 That Were Isolated from Reactions of (DⁱPPBIAN)CoBr₂ and LiEt₃BH

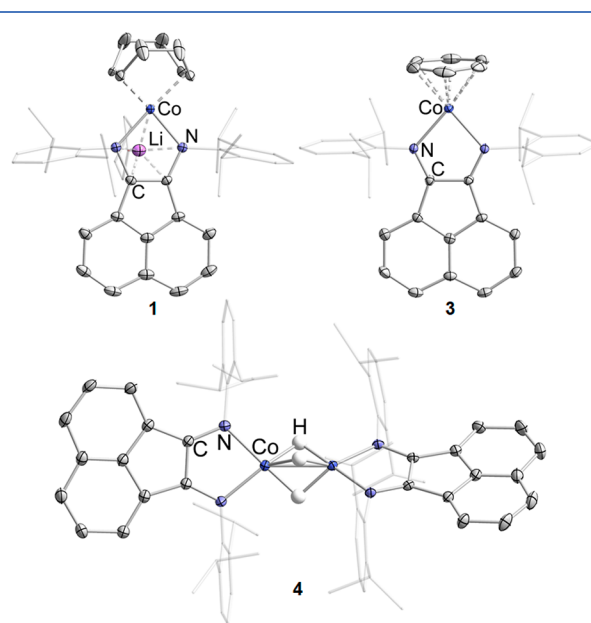
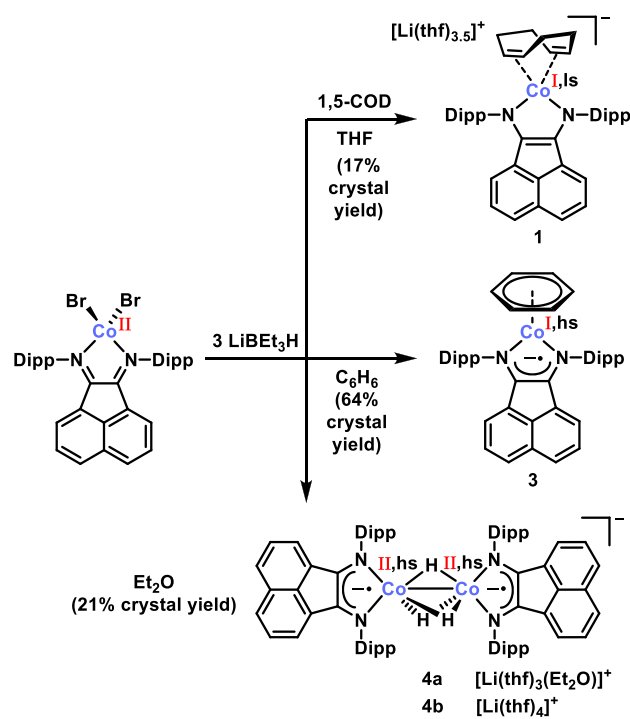


Figure 2. Molecular structures of 1, 3, and 4b. Thermal ellipsoids at the 50% probability level; minor disordered parts, noncoordinated solvents, selected H atoms, and the [Li(thf)₄]⁺ cation of 4b were omitted for clarity.

2), which was further investigated by EPR.^{28,29} The X-band spectrum of 3 in toluene glass at 20 K (Figure 3) shows a rhombic symmetry and was simulated in accordance with an unpaired electron coupled to a spin 7/2 nucleus. We attribute this signal to a cobalt-centered radical (SI). Inclusion of the Euler angles [−2.0, +90.0, 0] proved to be necessary to align the *g* and *A*_{Co} tensors and provided a more satisfactory simulation of the measured spectrum. Some linear and quadratic *A*-strain parameters have been included to simulate

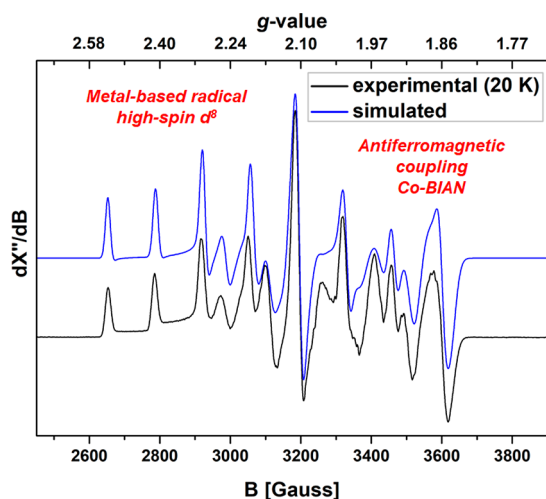


Figure 3. Simulated (blue) and experimental (black) X-band EPR spectrum of **3** in toluene glass at 20 K. $\nu = 9.389494$ GHz, microwave power = 1.002 mW, mod amp = 1.000 G.

the final line shape (SI). Some remaining slight deviations in the line shapes between simulation and experiment can be attributed to nonperfect glass formation. The provided simulation allowed for accurate determination of the g and A_{Co} tensors (MHz): [2.013, 2.145, 2.134] and [+185.0, +406.0, 198.4], respectively. These results are in agreement with an effective magnetic moment μ_{eff} of $1.9 \mu_{\text{B}}$ (Evans method, C_6D_6), which is only slightly higher than the spin-only value for an $S = 1/2$ system ($\mu_{\text{eff}} = 1.7 \mu_{\text{B}}$).

Further analysis of **3** included elemental analysis, LIFDI-MS ($m/z = 637.2781$), cyclic voltammetry (CV, one reversible reduction, $E = -2.3$ V vs Fc/Fc⁺), and UV-vis (C_6H_6 , $\lambda_{\text{max}} = 481$ nm, $\epsilon_{\text{max}} = 14300$ mol⁻¹ cm⁻¹ L). The combined data point to a highly unusual electronic structure of complex **3** which is described as a [(BIAN⁻)Co^I(η^6 -C₆H₆)] complex that contains a very rare high-spin Co(I) center.³¹ The BIAN radical anion is (strongly) antiferromagnetically coupled to the $S = 1$ Co(I) ion, thus resulting in an effective $S = 1/2$ system with the unpaired electron being primarily located at Co (as detected by EPR). The cobalt-arene coordination in **3** is not only relevant for the catalysis protocol, as it is structurally related to [(^DiPPBIAN)Co]₂. Moreover, substrates may coordinate in a similar way, as most substrates involve a phenyl ring. **3** also cocrystallized in a benzene-free synthesis of **1**, which might be a consequence of a solvent impurity.

Transition metal hydrides are key intermediates in many synthetic³² and biological³³ processes. The largest industrial catalytic processes are hydrogenation reactions that operate via metal hydride species. Since the landmark studies of homogeneous Rh-catalyzed hydrogenations,² extensive knowledge of hydridorhodium complexes has been collected whereas very little is known about the nature and catalytic role of related intermediates in Co-catalyzed reactions. From a reaction of (^DiPPBIAN)CoBr₂ with 3 equiv LiEt₃BH in Et₂O in a closed reaction vessel, we isolated a structurally unusual cobalt hydride complex (SI).³⁴ Effervescence was observed during the reduction, presumably by formation of H₂. Extraction with *n*-heptane and Et₂O afforded the anionic hydridocobaltate [Li(thf)₃(Et₂O){(^DiPPBIAN)Co}₂(μ -H)₃] (**4a**) as dark green microcrystals in 23% yield.³⁵ The closely related [Li(thf)₄]⁺ (**4b**) solvate can be isolated in an analogous fashion by crystallization from THF/*n*-hexane (Figure 2 and

SI). X-ray diffraction analysis revealed that **4a** and **4b** show very similar solid-state molecular structures, thus only the structural parameters of **4a** are given below. The anion of **4a** shows three hydride ligands (located in the electron density Fourier map) that bridge two (^DiPPBIAN)Co units (Figure 2). The [Li(thf)₃(Et₂O)]⁺ counterion is solvent-separated. A very short Co–Co distance presumably is observed due to the presence of three bridging hydrides: 2.2640(5) and 2.2426(3) Å for **4a** and **4b**, respectively. To the best of our knowledge, the latter is the shortest Co(μ -H)_nCo motif known to date (2nd shortest: 2.249(1) Å).^{35b} The Co–H bond distances are between 1.51(2) and 1.63(5) Å. The twist angle between the two CoN₂ planes is 54.94(7)°. The NCCN bond lengths of BIAN are slightly shorter than in **3** (Figure 1; C–N 1.333(3)–1.349(3) Å; C–C 1.412(3)–1.419(3) Å), yet are in good agreement with the monoanionic BIAN in the complex [(^DiPPBIAN)₂Fe] (C–N 1.3367(15) and 1.3393(15) Å; C–C 1.4234(18) Å) which contains a high-spin Fe²⁺ that is antiferromagnetically coupled to BIAN.³⁶ Accordingly, the observed bond lengths of the BIAN ligands in **4** suggest a radical anion state of BIAN which is supported by theoretical studies (*vide infra*).^{28,29,37}

The sum formula of **4a** was further verified by negative-ion mode ESI mass spectrometry (Figure 4, $m/z = 1121.4$). The

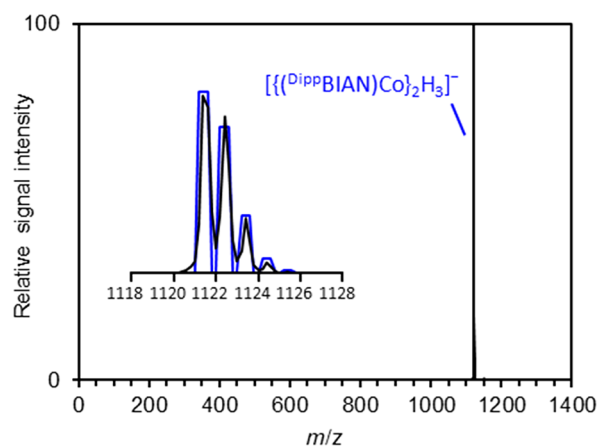


Figure 4. ESI-MS of **4a**. Negative-ion mode ESI mass spectrum of **4a** (5 mM in THF). (inset) Experimental (black) and simulated (blue line) isotope pattern of [({^DiPPBIAN)Co}₂H₃]⁻.

compound proved highly sensitive as unsealed THF solutions decomposed in an argon-filled glovebox within several hours to a red-brown paramagnetic mixture presumably by formation of H₂. Direct evidence of such decomposition came from the gas-phase fragmentation of the mass-selected anionic component of **4a** in ESI-MS. Apart from dissociation into its monomeric subunit [(^DiPPBIAN)CoH₂]⁻, the dinuclear cobaltate readily underwent dehydrogenation (Figures S25 and S26). Remarkably, multiple dehydrogenation steps were operative (≥ 7). Most likely, the released H atoms originated from the bridging hydrides and from the isopropyl groups of the ^DiPPBIANs. The ¹H NMR spectrum of **4a** displayed a characteristic, broad singlet resonance for the three bridging hydrides at -75.2 ppm (see the Supporting Information for 2D NMR analyses). This remarkable high-field shift may indicate an open-shell structure which was further investigated by temperature-dependent ¹H NMR studies.³⁸ The chemical shift of this resonance is temperature-dependent and shows a strong upfield shift upon

decreasing temperature (Figure 5). A similar behavior is observed for the remaining ^1H NMR resonances. The observed

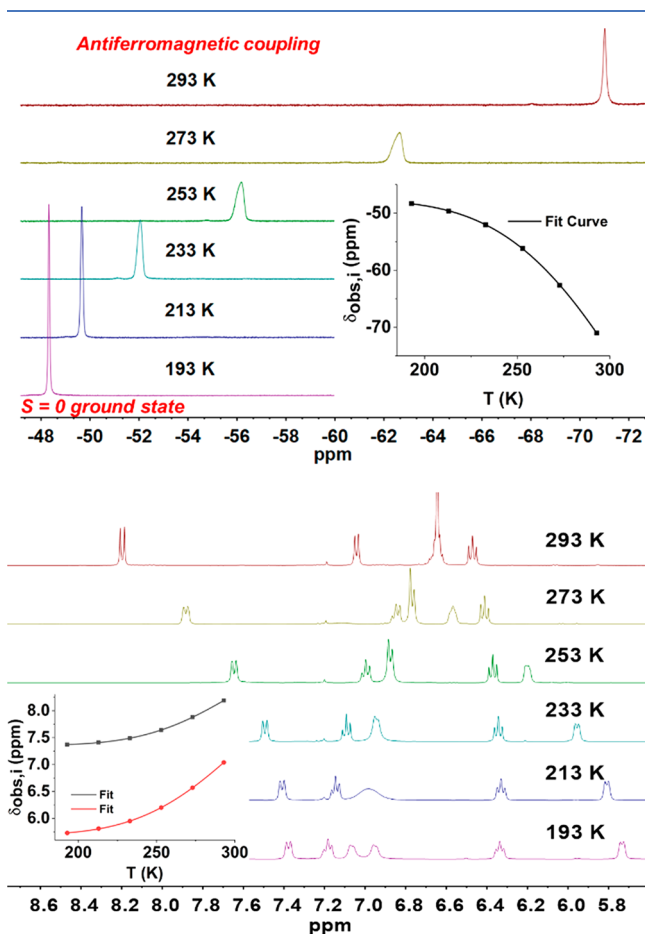


Figure 5. Variable temperature ^1H NMR spectrum of **4a**.

non-Curie behavior indeed points to an antiferromagnetic coupling of the cobalt centers with the diamagnetic ground state at low temperatures. Signal fitting provided a ratio of the coexisting configurations. Hence, the paramagnetic configurations are 27% of the singlet at 293 K (Figure 5 and SI).⁵⁹ The ratio decreased to 0.3% at 193 K ($\Delta E_{\text{triplet-singlet}} = 21.4$ kJ/mol). An effective magnetic moment $\mu_{\text{eff}} = 2.1 \mu_{\text{B}}$ per dimer was determined in solution at 293 K (Evans method, THF- d_8).

The solid-state magnetic behavior of the crystalline sample of **4b** was investigated in the 2–250 K range by SQUID magnetometry (Figure 6). The $\chi_{\text{M}}T$ product was $1.76 \text{ cm}^3 \text{ mol}^{-1} \text{ K}$ (or $3.75 \mu_{\text{B}}$) at 250 K and decreased to almost zero by lowering the temperature, indicating overall antiferromagnetic coupling and a diamagnetic ground state of **4b**. The best fit was achieved using a model of four antiferromagnetically coupled centers: two BIAN radical anions with $S = 1/2$ and two $S = 3/2$ cobalt(II) ions. The best fit parameters were the following: $g(\text{BIAN}) = 2.0$ (fixed), $g(\text{Co(II)}) = 2.08$, $J(\text{BIAN-Co}) = -427 \text{ cm}^{-1}$ and $J(\text{Co-Co}) = -17 \text{ cm}^{-1}$.

Additional analyses of the cobaltate **4a** include elemental analysis (EA), UV-vis spectroscopy (C_6H_6 , $I_{\text{max}} = 474 \text{ nm}$, $\epsilon_{\text{max}} = 1200 \text{ mol}^{-1} \text{ cm}^{-1} \text{ L}$), and cyclic voltammetry (THF/ $[\text{nBu}_4\text{N}]\text{PF}_6$; one reversible reduction was observed $E = -2.4 \text{ V vs Fc/Fc}^+$). The combined data are strongly indicative of a highly unusual electronic structure of the trihydridocobaltate anion of **4a,b**, which is best described as $[\{(\text{DippBIAN})-$

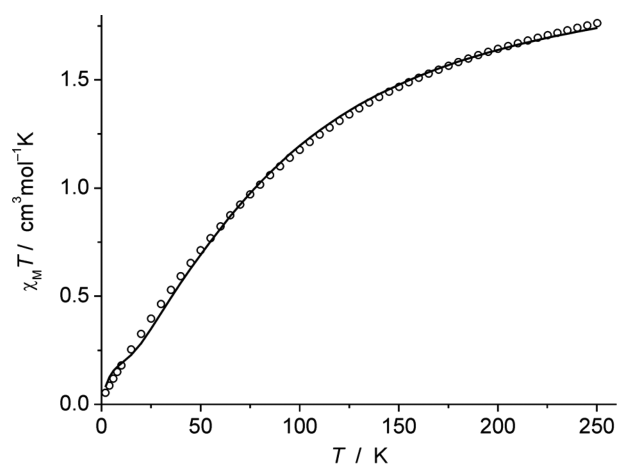


Figure 6. Temperature-dependence of the product $\chi_{\text{M}}T$ of **4b**.

$\text{Co}^{\text{II}}\}_{2}(\mu\text{-H})_3]^{-1}$, assuming that DippBIAN and each bridging hydride atom are singly negatively charged, respectively. DFT calculations suggest a charge of -0.33 for each of the hydrides and of 0.85 for each of the cobalt centers (Figure 7). Since

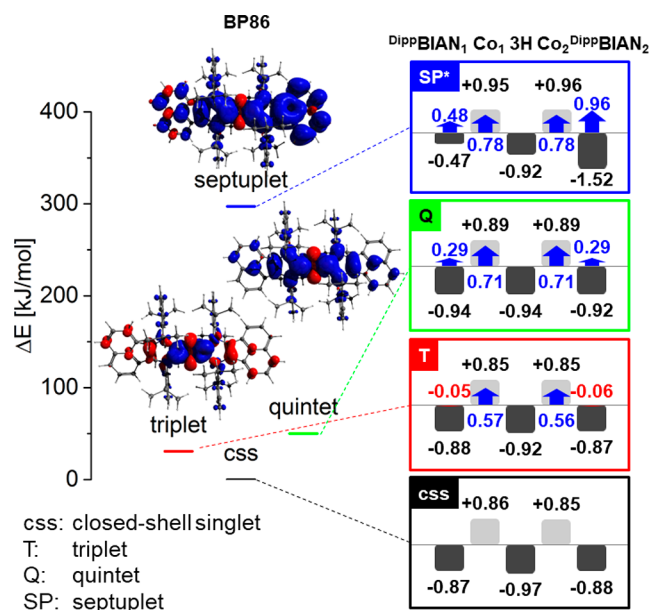
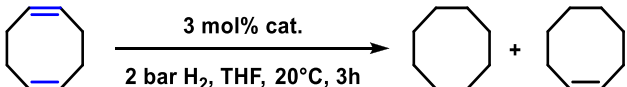


Figure 7. Energy diagram of **4** in various spin states. Anion optimized with BP86/def2-TZVP. (left) Spin density (isosurface value: 0.001) of the corresponding spin state. (right) Local charges (light/dark gray: positive/negative) and spins (blue/red: α/β) on specific fragments of the molecule in different spin states. A local spin of $1/2$ corresponds to one unpaired electron. * From single-point calc on optimized mol structure in css state (BP86/def2-TZVP).

charge distributions are typically less polarized than formal oxidation numbers suggest, this is compatible with a Co^{II} assignment, even though it does not exclude Co^{I} . Importantly, DFT confirms the singlet ground state, this state being both lowest in energy and showing the best agreement with the X-ray crystallographic structure.³⁷

Hydrogenation Activities of Complexes 1–4 and Mechanistic Proposal. We evaluated the catalytic activities of the isolated cobalt complexes **1–4** and various precatalyst mixtures in a hydrogenation model reaction (Table 2). The cobaltate complex $[\text{Li}(\text{thf})_{3,5}\{\text{DippBIAN}\}\text{Co}(\text{cod})]$ (**1**) was

Table 2. Hydrogenations with Isolated Complexes and Precatalyst Mixtures^a


entry	catalyst mixture	yield [%] ^b	
		cyclo-octane	cyclo-octene
1 ^c	(^{Dipp} BIAN)CoBr ₂ + 9 mol % LiBEt ₃ H	96	1
2	[Li(thf) _{3,5} {(^{Dipp} BIAN)Co(cod)}] 1	5	61
3	1 + 3.5 mol % 12-crown-4	4	44
4	1 + 3 mol % [Fc]PF ₆	2	17
5	1 + 9 mol % BEt ₃	66	33
6	[K(thf){(^{Dipp} BIAN)Co(cod)}] 2		1
7	2 + 3 mol % [Fc]PF ₆	1	
8	2 + 30 mol % LiBr + [2.2.2]Cryptand		2
9	2 + 30 mol % LiCl + 3 mol % 18-crown-6		1
10	2 + 9 mol % BEt ₃	1	1
11	2 + 9 mol % BEt ₃ + 30 mol % LiBr	3	38
12 ^c	[Li(thf) ₃ (Et ₂ O){(^{Dipp} BIAN)Co} ₂ (μ ² -H) ₃] 4a	6	7
13 ^c	4a + 3 mol % Et ₃ B	22	22
14 ^c	4a + 1.5 mol % LiEt ₃ BH	57	43
15	[(^{Dipp} BIAN)Co(η ⁶ -C ₆ H ₆)] 3		
16 ^d	3 + 9 mol % LiBEt ₃ H	4	29

^aConditions: 0.2 mmol alkene, 0.1 M in THF, 3 mol % cat, 2 bar H₂.

^bYields determined by quantitative GC-FID vs internal *n*-pentadecane; ane = cyclooctane, ene = cyclooctene. ^c1.5 mol % 4a.

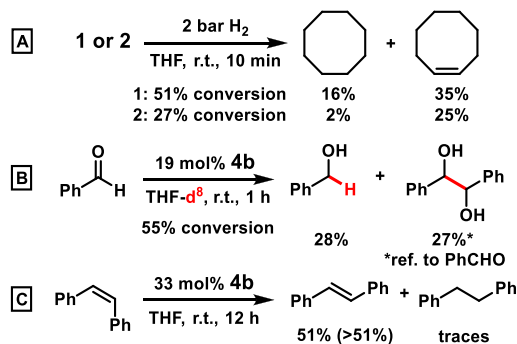
^dReduction in the presence of the substrate.

found to be active for the hydrogenation of 1,5-cyclooctadiene (cod), albeit exhibiting slightly lower activity than the *in situ* formed catalyst (entry 2). Interestingly, 1 could be further activated by addition of 3 equiv Et₃B (entry 5), which may indicate Lewis acid-assisted catalysis.⁴⁰ The borane could facilitate the cleavage of H₂ as demonstrated by Peters and co-workers with a borylcobalt complex.^{40a} The catalytic inactivity of the corresponding potassium derivative [K(thf){(^{Dipp}BIAN)Co(cod)}] (2, Table 2, entry 6) manifested the observed alkali cation effect during our preliminary optimization experiments (Table 1, entries 1 and 5, and SI).¹⁹ One possible explanation for this effect is an attractive noncovalent cation-π interaction. As mainly an electrostatic interaction, the association free enthalpy (Δ*H*^o) for the alkali metals with benzene follows the trend: Li⁺ > Na⁺ > K⁺. Hence, the alkali cation can stabilize transition states or bind substrates (i.e., alkenes, arenes) in proximity to the catalyst.¹⁹ Moreover, alkali metals are able to tune the redox activity of the ligand. Mazzanti and co-workers reported on ligand- or metal-based reduction of cobalt salophen complexes dependent on the alkali metal.^{19f} The group of Holland reported reduced iron dimers with redox-active formazanate ligands. The dimer, which is stabilized by cation-π interactions, rearranged in THF solution to form a five-membered metallacycle with a reactivity order of Na⁺ > K⁺ < Rb⁺ < Cs⁺.^{19h}

The neutral (benzene)cobalt complex [(^{Dipp}BIAN)Co(η⁶-C₆H₆)] 3 was only active after additional reduction with LiEt₃BH (Table 2, entry 16). Notably, the related 17 valence electron (VE) complex [(dppe)Co(cod)] (dppe = 1,2-diphenylphosphinoethane) bearing a redox-innocent ligand is indeed an active precatalyst for hydrogenations.^{8d} The hydridocobaltate [Li(thf)₃(Et₂O){(^{Dipp}BIAN)Co}₂(μ-H)₃] (4a) showed moderate hydrogenation activity which was

significantly enhanced by further reduction with 0.5 equiv of LiEt₃BH (entries 12 and 14). It may be speculated that the hydridocobaltate anion present in 4a,b (or related derivatives) acts as a catalyst reservoir for mononuclear hydrides as indicated by *in situ* NMR studies (SI). A catalytic mechanism via multinuclear metal complexes can likely be ruled out (first order in [Co], poisoning studies, SI).⁴¹ Based on the collected synthetic, spectroscopic, and theoretical data, we propose a homotopic reaction mechanism that involves cobaltate complexes as active catalyst species. Rate acceleration by Lewis acids and an alkali-cation effect were observed.

The observed alkali cation effect was also evident in the more effective stoichiometric hydrogenation of 1 vs 2 (Scheme 6, A). Preliminary explorations of the reactivity of relevant

Scheme 6. Related Reactivity of 1, 2, and 4b

hydrides were performed with 4b as model compound: Protolysis occurred with the strong Brønsted acid HCl in dioxane to give H₂ evolution (2.3 ± 0.1 equiv H₂). In the presence of benzaldehyde, 4b reacted to give 28% benzyl alcohol and 27% pinacol coupling product (Scheme 6B). This may indicate the competing operation of hydride transfer and single-electron transfer processes from 4b. In the absence of dihydrogen, incomplete isomerization of (*Z*)-stilbene to (*E*)-stilbene was observed (51%, Scheme 6C). 4a represents a conceivable intermediate in our recently published (BIAN)Co-catalyzed amine-borane dehydrogenation reaction as it affords the same reaction products (borazine, cyclotriaminoborane, cyclodiaminoborane, H₃BNH₂-cyclo-B₃N₃H₁₁, polyborazine, and polyaminoborane; SI).^{16e}

CONCLUSION

In summary, this report has established reduced cobalt complexes as competent catalysts in a user-friendly hydrogenation protocol for challenging alkenes under mild conditions. The obtained reactivity suggests bidentate BIANs as interesting alternatives to well-established pincer-type motifs possessing comparably high activities in cobalt-catalyzed alkene and imine hydrogenations. Mechanistic studies revealed considerable alkali-cation and Lewis-acid effects. Synthetic, kinetic, and spectroscopic experiments indicate a mechanism involving homotopic cobaltate catalysts. Catalytically relevant cobalt complexes were isolated that document the redox noninnocence of the BIAN ligand. Especially, the isolation of trihydridocobaltates 4a,b represents a tangible advance over the current state-of-the-art of transition metal hydrides. Their molecular structures show the first reported anionic cobalt complex with bridging hydride ligands. In contrast to the vast majority of reported transition metal hydrides bearing

multidentate phosphines, cyclopentadienyl, or carbonyl ligands, the high electron density in this complex is stabilized by the redox noninnocent BIAN. It is reasonable to assume that the anion in **4a,b** constitutes a catalytically competent off-cycle intermediate of (BIAN)Co-catalyzed (de)hydrogenation reactions.^{16e}

■ ASSOCIATED CONTENT

● Supporting Information

The Supporting Information is available free of charge on the ACS Publications website at DOI: 10.1021/acscatal.9b01584.

Experimental procedures, analytical and crystal data of compounds, mechanistic studies, and spectra (PDF)

Combined crystal data for (^DiPPBIAN)CoBr₂, **1**, **3**, **4a**, **4b** with CCDC 1909828, 1909827, 1909829, 1909830, 1909831, respectively (CIF)

Individual CIFs and reports for (^DiPPBIAN)CoBr₂, **1**, **3**, **4a**, and **4b** (ZIP)

■ AUTHOR INFORMATION

Corresponding Authors

*E-mail: axel.jacobi@uni-hamburg.de (A.J.v.W.).

*E-mail: robert.wolf@ur.de (R.W.).

ORCID

Konrad Koszinowski: 0000-0001-7352-5789

Bas de Bruin: 0000-0002-3482-7669

Franz Meyer: 0000-0002-8613-7862

Robert Wolf: 0000-0003-4066-6483

Axel Jacobi von Wangelin: 0000-0001-7462-0745

Notes

The authors declare no competing financial interest.

■ ACKNOWLEDGMENTS

We thank Prof. Jürgen Heck, Prof. Peter Burger, and Dr. Dieter Schaarschmidt for helpful discussions. Technical assistance by Max Völker, Felix Seeberger, and Ursula Otterpohl is gratefully acknowledged. This work was financed by the Deutsche Forschungsgemeinschaft (DFG, JA 1107/6-1, WO 1496/6-1, KK 2875/8-1), the European Research Council (ERC, CoG 683150), and the Fonds der Chemischen Industrie (T.M.M.).

■ REFERENCES

- (1) (a) Nishimura, S. *Handbook of Heterogeneous Catalytic Hydrogenation for Organic Synthesis*; Wiley: New York, 2001. (b) *The Handbook of Homogeneous Hydrogenation*; de Vries, J. G.; Elsevier, C. J., Eds.; Wiley-VCH: Weinheim, 2007.
- (2) (a) Meakin, P.; Jesson, J. P.; Tolman, C. A. The Nature of Chlorotris(triphenylphosphine)Rhodium in Solution and Its Reaction with Hydrogen. *J. Am. Chem. Soc.* **1972**, *94*, 3240–3242. (b) Tolman, C. A.; Meakin, P. Z.; Lindner, D. L.; Jesson, J. P. Triarylphosphine, Hydride, and Ethylene Complexes of Rhodium(I) Chloride. *J. Am. Chem. Soc.* **1974**, *96*, 2762–2774. (c) Halpern, J. Mechanistic Aspects of Homogeneous Catalytic Hydrogenation and Related Processes. *Inorg. Chim. Acta* **1981**, *50*, 11–19. (d) Halpern, J. Mechanism and Stereoselectivity of Asymmetric Hydrogenation. *Science* **1982**, *217*, 401–407. (e) Duckett, S. B.; Newell, C. L.; Eisenberg, R. Observation of New Intermediates in Hydrogenation Catalyzed by Wilkinson's Catalyst, RhCl(PPh₃)₃, Using Parahydrogen-Induced Polarization. *J. Am. Chem. Soc.* **1994**, *116*, 10548–10556.
- (3) Bullock, R. M. *Catalysis without Precious Metals*; Wiley-VCH: Weinheim, Germany, 2010.
- (4) (a) Hess, W.; Treutwein, J.; Hilt, G. Cobalt-Catalyzed Carbon-Carbon Bond-Formation Reactions. *Synthesis* **2008**, *40*, 3537–3562.

- (b) Holzwarth, M. S.; Plietker, B. Biorelevant Metals in Sustainable Metal Catalysis-A Survey. *ChemCatChem* **2013**, *5*, 1650–1679.
- (c) Röse, P.; Hilt, G. Cobalt-Catalyzed Bond Formation Reactions; Part 2. *Synthesis* **2016**, *48*, 463–492.

(5) *Non-Noble Metal Catalysis: Molecular Approaches and Reactions*; Klein Gebbink, R. J. M.; Moret, M.-E., Eds.; Wiley-VCH: Weinheim, Germany, 2019.

- (6) Efficient heterogeneous Co catalysts have been prepared by chemical reduction, pyrolysis, or solvothermal synthesis: (a) Chen, F.; Topf, C.; Radnik, J.; Kreyenschulte, C.; Lund, H.; Schneider, M.; Surkus, A. E.; He, L.; Junge, K.; Beller, M. Stable and Inert Cobalt Catalysts for Highly Selective and Practical Hydrogenation of C≡N and C = O Bonds. *J. Am. Chem. Soc.* **2016**, *138*, 8781–8788. (b) Wei, Z.; Chen, Y.; Wang, J.; Su, D.; Tang, M.; Mao, S.; Wang, Y. Cobalt Encapsulated in N-Doped Graphene Layers: An Efficient and Stable Catalyst for Hydrogenation of Quinoline Compounds. *ACS Catal.* **2016**, *6*, 5816–5822. (c) Jagadeesh, R. V.; Murugesan, K.; Alshammari, A. S.; Neumann, H.; Pohl, M.-M.; Radnik, J.; Beller, M. MOF-Derived Cobalt Nanoparticles Catalyze a General Synthesis of Amines. *Science* **2017**, *358*, 326–332. (d) Sandl, S.; Schwarzhuber, F.; Pöllath, S.; Zweck, J.; Jacobi von Wangelin, A. Olefin-Stabilized Cobalt Nanoparticles for C = C, C = O, and C = N Hydrogenations. *Chem. - Eur. J.* **2018**, *24*, 3403–3407. (e) Büschelberger, P.; Reyes-Rodríguez, E.; Schöttle, C.; Treptow, J.; Feldmann, C.; Jacobi von Wangelin, A.; Wolf, R. Recyclable Cobalt(0) Nanoparticle Catalysts for Hydrogenations. *Catal. Sci. Technol.* **2018**, *8*, 2648–2653.

(7) Reviews: (a) Chirik, P. J. Iron- and Cobalt-Catalyzed Alkene Hydrogenation: Catalysis with Both Redox-Active and Strong Field Ligands. *Acc. Chem. Res.* **2015**, *48*, 1687–1695. (b) Zell, T.; Langer, R. From Ruthenium to Iron and Manganese-A Mechanistic View on Challenges and Design Principles of Base-Metal Hydrogenation Catalysts. *ChemCatChem* **2018**, *10*, 1930–1940. (c) Mukherjee, A.; Milstein, D. Homogeneous Catalysis by Cobalt and Manganese Pincer Complexes. *ACS Catal.* **2018**, *8*, 11435–11469. (d) Papa, V.; Junge, K.; Beller, M. Cobalt-Pincer Complexes in Catalysis. *Chem. - Eur. J.* **2019**, *25*, 122–143. (e) Alig, L.; Fritz, M.; Schneider, S. First-Row Transition Metal (De)Hydrogenation Catalysis Based On Functional Pincer Ligands. *Chem. Rev.* **2019**, *119*, 2681–2751. (f) Ai, W.; Zhong, R.; Liu, X.; Liu, Q. Hydride Transfer Reactions Catalyzed by Cobalt Complexes. *Chem. Rev.* **2019**, *119*, 2876–2953.

(8) Selected examples: (a) Knijnenburg, Q.; Horton, A. D.; Van Der Heijden, H.; Kooistra, T. M.; Hetterscheid, D. G. H.; Smits, J. M. M.; De Bruin, B.; Budzelaar, P. H. M.; Gal, A. W. Olefin Hydrogenation Using Diimine Pyridine Complexes of Co and Rh. *J. Mol. Catal. A: Chem.* **2005**, *232*, 151–159. (b) Zhang, G.; Scott, B. L.; Hanson, S. K. Mild and Homogeneous Cobalt-Catalyzed Hydrogenation of C = C, C = O, and C = N Bonds. *Angew. Chem., Int. Ed.* **2012**, *51*, 12102–12106. (c) Yu, R. P.; Darmon, J. M.; Milsman, C.; Margulieux, G. W.; Stieber, S. C. E.; Debeer, S.; Chirik, P. J. Catalytic Hydrogenation Activity and Electronic Structure Determination of Bis(arylimidazol-2-ylidene)pyridine Cobalt Alkyl and Hydride Complexes. *J. Am. Chem. Soc.* **2013**, *135*, 13168–13184. (d) Friedfeld, M. R.; Margulieux, G. W.; Schaefer, B. A.; Chirik, P. J. Bis(phosphine)cobalt Dialkyl Complexes for Directed Catalytic Alkene Hydrogenation. *J. Am. Chem. Soc.* **2014**, *136*, 13178–13181. (e) Rösler, S.; Obenauf, J.; Kempe, R. A Highly Active and Easily Accessible Cobalt Catalyst for Selective Hydrogenation of C = O Bonds. *J. Am. Chem. Soc.* **2015**, *137*, 7998–8001. (f) Xu, R.; Chakraborty, S.; Yuan, H.; Jones, W. D. Acceptorless, Reversible Dehydrogenation and Hydrogenation of N-Heterocycles with a Cobalt Pincer Catalyst. *ACS Catal.* **2015**, *5*, 6350–6354. (g) Korstanje, T. J.; van der Vlugt, J. I.; Elsevier, C. J.; de Bruin, B. Hydrogenation of Carboxylic Acids with a Homogeneous Cobalt Catalyst. *Science* **2015**, *350* (6258), 298–302. (h) Adam, R.; Cabrero-Antonino, J. R.; Spannenberg, A.; Junge, K.; Jackstell, R.; Beller, M. A General and Highly Selective Cobalt-Catalyzed Hydrogenation of N-Heteroarenes under Mild Reaction Conditions. *Angew. Chem., Int. Ed.* **2017**, *56*, 3216–3220.

(9) (a) Lyaskovskyy, V.; de Bruin, B. Redox Non-Innocent Ligands: Versatile New Tools to Control Catalytic Reactions. *ACS Catal.* **2012**,

2, 270–279. (b) Luca, O. R.; Crabtree, R. H. Redox-Active Ligands in Catalysis. *Chem. Soc. Rev.* **2013**, *42*, 1440–1459.

(10) (a) Gärtner, D.; Welther, A.; Rad, B. R.; Wolf, R.; Jacobi von Wangelin, A. Heteroatom-Free Arene-Cobalt and Arene-Iron Catalysts for Hydrogenations. *Angew. Chem., Int. Ed.* **2014**, *53*, 3722–3726. (b) Büschelberger, P.; Gärtner, D.; Reyes-Rodriguez, E.; Kreyenschmidt, F.; Koszinowski, K.; Jacobi von Wangelin, A.; Wolf, R. Alkene Metalates as Hydrogenation Catalysts. *Chem. - Eur. J.* **2017**, *23*, 3139–3151.

(11) Schnöckelborg, E. M.; Khusniyarov, M. M.; De Bruin, B.; Hartl, F.; Langer, T.; Eul, M.; Schulz, S.; Pöttgen, R.; Wolf, R. Unraveling the Electronic Structures of Low-Valent Naphthalene and Anthracene Iron Complexes: X-Ray, Spectroscopic, and Density Functional Theory Studies. *Inorg. Chem.* **2012**, *51*, 6719–6730.

(12) tom Dieck, H.; Bruder, H. Bis(diazadiene)Iron Complexes, $(R^1N = CR^2 - CR^2 = NR^1)_2Fe$. *J. Chem. Soc., Chem. Commun.* **1977**, 24–25.

(13) Flisak, Z.; Sun, W. H. Progression of Diiminopyridines: From Single Application to Catalytic Versatility. *ACS Catal.* **2015**, *5*, 4713–4724.

(14) (a) Hill, N. J.; Vargas-Baca, I.; Cowley, A. H. Recent Developments in the Coordination Chemistry of Bis(imino)acenaphthene (BIAN) Ligands with s- and p-Block Elements. *Dalton Trans.* **2009**, 240–253. (b) Fedushkin, I. L.; Skatova, A. A.; Chudakova, V. A.; Fukin, G. K. Four-Step Reduction of Dpp-Bian with Sodium Metal: Crystal Structures of the Sodium Salts of the Mono-, Di-, Tri- and Tetraanions of Dpp-Bian. *Angew. Chem., Int. Ed.* **2003**, *42*, 3294–3298.

(15) Selected examples of hydrogenations with BIAN: (a) van Asselt, R.; Elsevier, C. J. Homogeneous Catalytic Hydrogenation of Alkenes by Zero-Valent Palladium Complexes of Cis-Fixed Dinitrogen Ligands. *J. Mol. Catal.* **1991**, *65*, L13–L19. (b) Van Laren, M. W.; Elsevier, C. J. Selective Homogeneous Palladium(0)-Catalyzed Hydrogenation of Alkynes to (Z)-Alkenes. *Angew. Chem., Int. Ed.* **1999**, *38* (24), 3715–3717. (c) Villa, M.; Miesel, D.; Hildebrandt, A.; Ragaini, F.; Schaarschmidt, D.; Jacobi von Wangelin, A. Synthesis and Catalysis of Redox-Active Bis(imino)acenaphthene (BIAN) Iron Complexes. *ChemCatChem* **2017**, *9*, 3203–3209.

(16) Selected (BIAN)Co reports: (a) Khusniyarov, M. M.; Harms, K.; Burghaus, O.; Sundermeyer, J. Molecular and Electronic Structures of Homoleptic Nickel and Cobalt Complexes with Non-Innocent Bulky Diimine Ligands Derived from Fluorinated 1,4-Diazabuta-1,3-Butadiene (DAD) and Bis(arylimino)acenaphthene (BIAN). *Eur. J. Inorg. Chem.* **2006**, *2006*, 2985–2996. (b) Rosa, V.; Carabineiro, S. A.; Avilés, T.; Gomes, P. T.; Welter, R.; Campos, J. M.; Ribeiro, M. R. Synthesis, Characterisation and Solid State Structures of α -Diimine Cobalt(II) Complexes: Ethylene Polymerisation Tests. *J. Organomet. Chem.* **2008**, *693*, 769–775. (c) Pelties, S.; Maier, T.; Herrmann, D.; De Bruin, B.; Rebreyend, C.; Gärtner, S.; Shenderovich, I. G.; Wolf, R. Selective P_4 Activation by a Highly Reduced Cobaltate: Synthesis of Dicobalt Tetrakisphosphido Complexes. *Chem. - Eur. J.* **2017**, *23*, 6094–6102. (d) Formenti, D.; Ferretti, F.; Topf, C.; Surkus, A.-E.; Pohl, M.-M.; Radnik, J.; Schneider, M.; Junge, K.; Beller, M.; Ragaini, F. Co-Based Heterogeneous Catalysts from Well-Defined α -Diimine Complexes: Discussing the Role of Nitrogen. *J. Catal.* **2017**, *351*, 79–89. (e) Maier, T. M.; Sandl, S.; Shenderovich, I. G.; Jacobi von Wangelin, A.; Weigand, J. J.; Wolf, R. Amine-Borane Dehydrogenation and Transfer Hydrogenation Catalyzed by α -Diimine Cobaltates. *Chem. - Eur. J.* **2019**, *25*, 238–245. (f) Ziegler, C. G. P.; Maier, T. M.; Pelties, S.; Taube, C.; Hennersdorf, F.; Ehlers, A. W.; Weigand, J. J.; Wolf, R. Construction of Alkyl-Substituted Pentaphosphido Ligands in the Coordination Sphere of Cobalt. *Chem. Sci.* **2019**, *10*, 1302–1308.

(17) Recent studies from our group showing the beneficial effect of olefins: (a) Gülak, S.; Jacobi von Wangelin, A. Chlorostyrenes in Iron-Catalyzed Biaryl Coupling Reactions. *Angew. Chem., Int. Ed.* **2012**, *51*, 1357–1361. (b) Gülak, S.; Gieshoff, T. N.; Jacobi von Wangelin, A. Olefin-Assisted Iron-Catalyzed Alkylation of Aryl Chlorides. *Adv. Synth. Catal.* **2013**, *355*, 2197–2202. (c) Gülak, S.; Stepanek, O.;

Malberg, J.; Rad, B. R.; Kotora, M.; Wolf, R.; Jacobi von Wangelin, A. Highly Chemoselective Cobalt-Catalyzed Biaryl Coupling Reactions. *Chem. Sci.* **2013**, *4*, 776–784.

(18) (a) Johnson, J. B.; Rovis, T. More than Bystanders: The Effect of Olefins on Transition-Metal-Catalyzed Cross-Coupling Reactions. *Angew. Chem., Int. Ed.* **2008**, *47*, 840–871. (b) Defieber, C.; Grützmacher, H.; Carreira, E. M. Chiral Olefins as Steering Ligands in Asymmetric Catalysis. *Angew. Chem., Int. Ed.* **2008**, *47*, 4482–4502.

(19) Cation effects: (a) Collman, J. P.; Finke, R. G.; Cawse, J. N.; Brauman, J. I. Lewis Acid Catalyzed $[RFe(CO)_4]^-$ Alkyl Migration Reactions. A Mechanistic Investigation. *J. Am. Chem. Soc.* **1978**, *100*, 4766–4772. (b) Hartmann, R.; Chen, P. Noyori's Hydrogenation Catalyst Needs a Lewis Acid Cocatalyst for High Activity. *Angew. Chem., Int. Ed.* **2001**, *40*, 3581–3585. (c) Macchioni, A. Ion Pairing in Transition-Metal Organometallic Chemistry. *Chem. Rev.* **2005**, *105*, 2039–2073. (d) Kennedy, C. R.; Lin, S.; Jacobsen, E. N. The Cation- π Interaction in Small-Molecule Catalysis. *Angew. Chem., Int. Ed.* **2016**, *55*, 12596–12624. (e) Kita, M. R.; Miller, A. J. M. An Ion-Responsive Pincer-Crown Ether Catalyst System for Rapid and Switchable Olefin Isomerization. *Angew. Chem., Int. Ed.* **2017**, *56*, 5498–5502. (f) Andrez, J.; Guidal, V.; Scopelliti, R.; Pécaut, J.; Gambarelli, S.; Mazzanti, M. Ligand and Metal Based Multielectron Redox Chemistry of Cobalt Supported by Tetradentate Schiff Bases. *J. Am. Chem. Soc.* **2017**, *139*, 8628–8638. (g) Neel, A. J.; Hilton, M. J.; Sigman, M. S.; Toste, F. D. Exploiting Non-Covalent π Interactions for Catalyst Design. *Nature* **2017**, *543*, 637–646. (h) Broere, D. L. J.; Mercado, B. Q.; Bill, E.; Lancaster, K. M.; Sproules, S.; Holland, P. L. Alkali Cation Effects on Redox-Active Formazanate Ligands in Iron Chemistry. *Inorg. Chem.* **2018**, *57*, 9580–9591. (i) Yamada, S. Cation- π Interactions in Organic Synthesis. *Chem. Rev.* **2018**, *118*, 11353–11432. (j) Mahmudov, K. T.; Gurbanov, A. V.; Guseinov, F. I.; Guedes da Silva, M. F. C. Noncovalent Interactions in Metal Complex Catalysis. *Coord. Chem. Rev.* **2019**, *387*, 32–46.

(20) α -Methylstyrene was hydrogenated under standard conditions in the presence of various functional additives (1 equiv, protocol B, 3 h, 20 °C, THF (2 mL)): No decrease in hydrogenation activity was observed with added $PhNH_2$, whereas reduced activity was observed with 4-Tol- CH_2OH and $PhC(O)Ph$, respectively. No conversion was obtained in the presence of $PhCN$, $PhC(O)H$, and $PhNO_2$, respectively (SI).

(21) Brenna, D.; Villa, M.; Gieshoff, T. N.; Fischer, F.; Hapke, M.; Jacobi von Wangelin, A. Iron-Catalyzed Cyclotrimerization of Terminal Alkynes by Dual Catalyst Activation in the Absence of Reductants. *Angew. Chem., Int. Ed.* **2017**, *56*, 8451–8454.

(22) Muthukrishnan, I.; Sridharan, V.; Menéndez, J. C. Progress in the Chemistry of Tetrahydroquinolines. *Chem. Rev.* **2019**, *119*, 5057–5191.

(23) (a) Widegren, J. A.; Finke, R. G. A review of the problem of distinguishing true homogeneous catalysis from soluble or other metal-particle heterogeneous catalysis under reducing conditions. *J. Mol. Catal. A: Chem.* **2003**, *198*, 317–341. (b) Astruc, D.; Lu, F.; Aranzas, J. R. Nanoparticles as Recyclable Catalysts: The Frontier between Homogeneous and Heterogeneous Catalysis. *Angew. Chem., Int. Ed.* **2005**, *44*, 7852–7872. (c) Crabtree, R. H. Resolving Heterogeneity Problems and Impurity Artifacts in Operationally Homogeneous Transition Metal Catalysts. *Chem. Rev.* **2012**, *112*, 1536–1554. (d) Drost, R. M.; Rosar, V.; Dalla Marta, S.; Lutz, M.; Demitri, N.; Milani, B.; de Bruin, B.; Elsevier, C. J. Pd-Catalyzed Z-Selective Semihydrogenation of Alkynes: Determining the Type of Active Species. *ChemCatChem* **2015**, *7*, 2095–2107.

(24) Kinetics and mechanism of the hydrogenation of α -cyclopropylstyrene (rate constant of the ring-opening rearrangement of the corresponding radical $3.6 \times 10^5 \text{ s}^{-1}$ at 22 °C in hexane solution): (a) Bullock, M. R.; Samsel, E. G. Hydrogen Atom Transfer Reactions of Transition-Metal Hydrides by Metal Carbonyl Hydrides. *J. Am. Chem. Soc.* **1990**, *112*, 6886–6898. (b) Choi, J.; Tang, L.; Norton, J. R. Kinetics of Hydrogen Atom Transfer from $(\eta^5-C_5H_5)Cr(CO)_3H$ to Various Olefins: Influence of Olefin Structure. *J. Am. Chem. Soc.* **2007**, *129*, 234–240. (c) de Bruin, B.; Dzik, W. I.; Li, S.; Wayland, B. B.

Hydrogen-Atom Transfer in Reactions of Organic Radicals with [Co^{II}(por)]. (por = Porphyrinato) and in Subsequent Addition of [Co(H)(por)] to Olefins. *Chem. - Eur. J.* **2009**, *15*, 4312–4320.

(25) (a) Anton, D. R.; Crabtree, R. H. Dibenzo[a,e]-cyclooctatetraene in a Proposed Test for Heterogeneity in Catalysts formed from Soluble Platinum-group Metal Complexes. *Organometallics* **1983**, *2*, 855–859. (b) Franck, G.; Brill, M.; Helmchen, G. Dibenzo[a,e]cyclooctene: Multi-gram Synthesis of a Bidentate Ligand. *Org. Synth.* **2014**, *89*, 55–65. (c) Sandl, S.; Jacobi von Wangelin, A. Dibenzo[a,e]cyclooctatetra-ene. In *Encyclopedia of Organic Reagents*; John Wiley & Sons: New York, USA, 2019.

(26) Yang, X.-J.; Fan, X.; Zhao, Y.; Wang, X.; Liu, B.; Su, J.-H.; Dong, Q.; Xu, M.; Wu, B. Synthesis and Characterization of Cobalt Complexes with Radical Anionic α -Diimine Ligands. *Organometallics* **2013**, *32*, 6945–6949.

(27) Examples of α -diimine cobaltates: (a) Li[(α -diimine)Co(cod)] Döring, M.; Uhlig, E.; Taldbach, T. Zur Reaktion von [Li(TMED)]₂ [Co(COD)]₂ mit π -Akzeptorliganden. *Z. Anorg. Allg. Chem.* **1991**, *600*, 163–167. (b) K[(bipy)Co(cod)] Brennessel, W. W.; Ellis, J. E. Naphthalene and Anthracene Cobaltates(1-): Useful Stable Sources of an Atomic Cobalt Anion. *Inorg. Chem.* **2012**, *51*, 9076–9094. (c) Na/Co/ α -diimine/polyarene complexes Wang, X.; Zhao, Y.; Gong, S.; Liu, B.; Li, Q.-S.; Su, J.-H.; Wu, B.; Yang, X.-J. Mono- and Dinuclear Heteroleptic Cobalt Complexes with α -Diimine and Polyarene Ligands. *Chem. - Eur. J.* **2015**, *21*, 13302–13310.

(28) Ray, K.; Petrenko, T.; Wiegardt, K.; Neese, F. Joint Spectroscopic and Theoretical Investigations of Transition Metal Complexes Involving Non-Innocent Ligands. *Dalton Trans.* **2007**, 1552–1566.

(29) For average bond distances of BIAN from the literature, see ref 16c: BIAN⁰ C–N 1.28, C–C 1.49; BIAN¹⁻ C–N 1.34, C–C 1.44; BIAN²⁻ C–N 1.39, C–C 1.40.

(30) Similar (η^6 -arene)Co complexes: (a) [(NacNac)Co(arene)] Dai, X.; Kapoor, P.; Warren, T. H. [Me₂NN]Co(η^6 -Toluene): O = O, N = N, and O = N Bond Cleavage Provides β -Diketiminato Cobalt μ -Oxo and Imido Complexes. *J. Am. Chem. Soc.* **2004**, *126*, 4798–4799. (b) [(α -diimine)Co(arene)] and [(α -diimine)Co]₂ See ref 26. (c) Cobalt α -diimine and polyarene complexes See ref 27c. (d) [(NacNac)Co(arene)] Chen, C.; Hecht, M. B.; Kavara, A.; Brennessel, W. W.; Mercado, B. Q.; Weix, D. J.; Holland, P. L. Rapid, Regioconvergent, Solvent-Free Alkene Hydrosilylation with a Cobalt Catalyst. *J. Am. Chem. Soc.* **2015**, *137*, 13244–13247. (e) [(α -diimine)Fe(arene)] complexes as inactive olefin hydrogenation precatalysts Bart, S. C.; Hawrelak, E. J.; Lobkovsky, E.; Chirik, P. J. Low-Valent α -Diimine Iron Complexes for Catalytic Olefin Hydrogenation. *Organometallics* **2005**, *24*, 5518–5527.

(31) Krzystek, J.; Ozarowski, A.; Zvyagin, S. A.; Telsler, J. High Spin Co(I): High-Frequency and -Field EPR Spectroscopy of CoX(PPh₃)₃ (X = Cl, Br). *Inorg. Chem.* **2012**, *51*, 4954–4964.

(32) Reviews: (a) Moore, D. S.; Robinson, S. D. Hydrido Complexes of the Transition Metals. *Chem. Soc. Rev.* **1983**, *12*, 415–452. (b) Darensbourg, M. Y.; Ash, C. E. Anionic Transition Metal Hydrides. *Adv. Organomet. Chem.* **1987**, *27*, 1–50. (c) Robinson, S. J. C.; Heinekey, D. M. Hydride & Dihydrogen Complexes of Earth Abundant Metals: Structure, Reactivity, and Applications to Catalysis. *Chem. Commun.* **2017**, *53*, 669–676.

(33) Reviews: (a) Lubitz, W.; Ogata, H.; Rüdiger, O.; Reijerse, E. Hydrogenases. *Chem. Rev.* **2014**, *114*, 4081–4148. (b) Schilter, D.; Camara, J. M.; Huynh, M. T.; Hammes-Schiffer, S.; Rauchfuss, T. B. Hydrogenase Enzymes and Their Synthetic Models: The Role of Metal Hydrides. *Chem. Rev.* **2016**, *116*, 8693–8749.

(34) It is noteworthy that the reaction needs to be performed in a closed reaction vessel as reported by Finke and co-workers: Laxson, W. W.; Özkar, S.; Folkman, S.; Finke, R. G. The Story of a Mechanism-Based Solution to an Irreproducible Synthesis Resulting in an Unexpected Closed-System Requirement for the LiBEt₃H-Based Reduction: The Case of the Novel Subnanometer Cluster, [Ir(1,5-COD)(μ -H)]₄, and the Resulting Improved, Independently Repeatable, Reliable Synthesis. *Inorg. Chim. Acta* **2015**, *432*, 250–257.

(35) Related hydrides: (a) Fryzuk, M. D.; Ng, J. B.; Rettig, S. J.; Huffman, J. C.; Jonas, K. Nature of the Catalytically Inactive Cobalt Hydride Formed upon Hydrogenation of Aromatic Substrates. Structure and Characterization of the Binuclear Cobalt Hydride [(Pr₂P(CH₂)₃PPt₂)Co]₂(H)(μ -H)₃. *Inorg. Chem.* **1991**, *30*, 2437–2441. (b) [(Cp*)Co]₂(μ^2 -H)₃ Kersten, J. L.; Rheingold, A. L.; Theopold, K. H.; Casey, C. P.; Widenhofer, R. A.; Hop, C. E. C. A. [Cp*Co = CoCp*]⁺ Is a Hydride. *Angew. Chem., Int. Ed. Engl.* **1992**, *31*, 1341–1343. (c) [(NacNac)Co(μ^2 -H)]₂ and K₂[(NacNac)Co(μ -H)]₂ Ding, K.; Brennessel, W. W.; Holland, P. L. Three-Coordinate and Four-Coordinate Cobalt Hydride Complexes That React with Dinitrogen. *J. Am. Chem. Soc.* **2009**, *131*, 10804–10805. (d) LiEt₃BH·[(dippe)Rh(μ_2 -H)]₂ Swartz, B. D.; Ateşin, T. A.; Grochowski, M. R.; Oster, S. S.; Brennessel, W. W.; Jones, W. D. Unusual Lithium Coordinated Platinum and Rhodium Hydride Dimers. *Inorg. Chim. Acta* **2010**, *363*, 517–522.

(36) Fedushkin, I. L.; Skatova, A. A.; Khvoynova, N. M.; Lukoyanov, A. N.; Fukin, G. K.; Ketkov, S. Y.; Maslov, M. O.; Bogomyakov, A. S.; Makarov, V. M. New High-Spin Iron Complexes Based on Bis(Imino)Acenaphthenes (BIAN): Synthesis, Structure, and Magnetic Properties. *Russ. Chem. Bull.* **2013**, *62*, 2122–2131.

(37) Based on molecular structure optimizations of the anion of **4a,b** with the BP86 functional and Ahlrichs' def2-TZVP basis set, the closed-shell singlet (css) represents the lowest energy state, with the triplet (t) being the next highest in energy ($\Delta E(t - \text{css}) = 30.8$ kJ/mol), followed by the quintet state (q) ($\Delta E(q - \text{css}) = 50.2$ kJ/mol; **SI**). Single-point energy calculations of the open-shell singlet state (oss) on the triplet molecular structure converged to the closed-shell singlet state (css). The highest energy state is the septuplet (sp) ($\Delta E(\text{sp} - \text{css}) = 297.2$ kJ/mol), which due to convergence issues is evaluated as a single-point energy calculation on the optimized molecular structure of the css. Molecular structure optimizations with the TPSSH functional and Ahlrichs' def2-TZVP basis set predict the triplet state to be the lowest energy state ($\Delta E(t - \text{css}) = 22.5$ kJ/mol), followed by the quintet state ($\Delta E(q - \text{css}) = 10.7$ kJ/mol; **SI**). From local charges and spins obtained from BADER population analysis, the cobalt ions in **4** are predicted to be singly positively charged for both the BP86 and TPSSH functional (**SI**). The three bridging hydrides summed up are singly negatively charged in total for either functional. The oxidation state of the BIAN core remains ambiguous, as its charge ranges between -1.15 (css) and -2.23 (t) and between -2.19 (oss) and -2.85 (t) for the BP86 and the TPSSH functional, respectively. However, the overall ligand fragment [^{Dippe}BIAN] turns out to be roughly singly negatively charged in all cases except for the septuplet.

(38) Knijnenburg, Q.; Hettterscheid, D.; Kooistra, T. M.; Budzelaar, P. H. M. The Electronic Structure of (Diiminopyridine)cobalt(I) Complexes. *Eur. J. Inorg. Chem.* **2004**, *2004*, 1204–1211.

(39) Bachmann, B.; Hahn, F.; Heck, J.; Wünsch, M. Cooperative Effects In π -Ligand Bridged Binuclear Complexes. 8. Cyclic Voltammetric, NMR, and ESR Spectroscopic Studies of Electron-Poor Syntactical Bis(η^5 -cyclopentadienyl)metal μ -Cyclooctatetraene Complexes of Chromium and Vanadium. *Organometallics* **1989**, *8*, 2523–2543.

(40) Lewis-acid effects in hydrogenation reactions: (a) Lin, T.-P.; Peters, J. C. Catalytic Boryl-Mediated Reversible H₂ Activation at Cobalt: Catalytic Hydrogenation, Dehydrogenation, and Transfer Hydrogenation. *J. Am. Chem. Soc.* **2013**, *135*, 15310–15313. (b) Maity, A.; Teets, T. S. Main Group Lewis Acid-Mediated Transformations of Transition-Metal Hydride Complexes. *Chem. Rev.* **2016**, *116*, 8873–8911. (c) Tokmic, K.; Jackson, B. J.; Salazar, A.; Woods, T. J.; Fout, A. R. Cobalt-Catalyzed and Lewis Acid-Assisted Nitrile Hydrogenation to Primary Amines: A Combined Effort. *J. Am. Chem. Soc.* **2017**, *139*, 13554–13561. (d) Léonard, N. G.; Chirik, P. J. Air-Stable α -Diimine Nickel Precatalysts for the Hydrogenation of Hindered, Unactivated Alkenes. *ACS Catal.* **2018**, *8*, 342–348.

(41) (a) Oro, L. A.; Sola, E. Mechanistic Aspects of Dihydrogen Activation and Catalysis by Dinuclear Complexes. In *Recent Advances in Hydride Chemistry*; Peruzzini, M., Poli, R., Eds.; Elsevier Science Ltd,

Amsterdam, Netherlands, 2001; pp 299–327. (b) Siedschlag, R. B.; Bernales, V.; Vogiatzis, K. D.; Planas, N.; Clouston, L. J.; Bill, E.; Gagliardi, L.; Lu, C. C. Catalytic Silylation of Dinitrogen with a Dicobalt Complex. *J. Am. Chem. Soc.* **2015**, *137*, 4638–4641. (c) Gieshoff, T. N.; Chakraborty, U.; Villa, M.; Jacobi von Wangelin, A. Alkene Hydrogenations by Soluble Iron Nanocluster Catalysts. *Angew. Chem., Int. Ed.* **2017**, *56*, 3585–3589. (d) Powers, I. G.; Uyeda, C. Metal-Metal Bonds in Catalysis. *ACS Catal.* **2017**, *7*, 936–958. (e) Chakraborty, U.; Reyes-Rodriguez, E.; Demeshko, S.; Meyer, F.; Jacobi von Wangelin, A. A Manganese Nanosheet: New Cluster Topology and Catalysis. *Angew. Chem., Int. Ed.* **2018**, *57*, 4970–4975.